Bioelectrochemistry 73 (2008) 97–100

Contents lists available at ScienceDirect

Bioelectrochemistry

journal homepage: www.elsevier.com/locate/bioelechem

Quantum mechanical scattering cross sections and permeability coefficients for ions crossing the human red cell and resting squid axon membranes

S.G. Elkomoss [a,*], I. Bernhardt [b], A. Pape [c]

[a] ULP - UFR de Sciences Physiques, 3-5 Rue de l'Université, F - 67084 Strasbourg Cedex 2, France
[b] Saarland University, Laboratory of Biophysics, House A2.4, P.O. Box 151150, D - 66041 Saarbruecken, Germany
[c] IPHC - UMR 7178 - CNRS - IN2P3/ULP, 23 Rue du Loess, BP 28, F - 67037 Strasbourg Cedex 2, France

ARTICLE INFO

Article history:
Received 5 June 2007
Received in revised form 18 December 2007
Accepted 4 March 2008
Available online 18 March 2008

Keywords:
Potential well
Elastic scattering cross section
Permeability coefficient
Human red blood cell
Resting axolemma squid axon

ABSTRACT

Quantum mechanical calculations of elastic scattering cross sections for some permeant ions crossing the human red blood cell and resting axolemma squid axon membranes have been carried out using the three-dimensional spherically symmetric square potential well. Making the assumption that the permeability coefficient is inversely proportional to scattering cross section, we obtain the order of membrane selectivity for the ions as well as values for the permeability coefficients. Despite the relatively simple method used, good agreement between calculated permeability coefficients and data available in the literature is obtained. We suggest that elastic scattering cross section measurements for ions in various membranes would be valuable not only because they give a precise idea about the permeability ratios between ions but they also determine the form of the potential the ions are moving in.

1. Introduction

In a preceding paper [1], the one-dimensional (1D) finite square potential well was used to calculate the transmission coefficients T_{calc} for some permeant neutral molecules crossing the human red blood cell (HRBC) and the resting axolemma squid axon membranes. Good agreement between T_{calc} and the experimental values T_{exp} was obtained. In the present work, the simplest three-dimensional (3D) spherically symmetric square potential well has been used for calculating elastic scattering cross sections σ and permeability coefficients P of permeant monovalent ions crossing these membranes. The ions treated here are HCO_3^-, Li^+, Cs^+, Cl^-, NH_4^+, K^+, Na^+ and Rb^+ for the HRBC. For the resting axolemma squid axon, K^+, Rb^+, Cl^-, Na^+ and NH_4^+ ions are considered. Due to the relatively simple approach used, the calculations of P for these ions can be considered in excellent agreement with the data available in the literature [2–13].

In contrast to classical physics, a distinctive feature of quantum mechanics (QM) is the existence of discrete bound states. They appear whenever a particle moves in a potential lower than its surroundings. This potential serves to attract particles [14] and hence properties such as transmission T, reflection $(1-T)$, σ, and P have a physical meaning and it should be possible to measure them. For instance, if one could measure σ for ions crossing various membranes, it should be possible to determine the potential these ions are moving in. This way a new line of research would be opened.

2. Calculations

2.1. The 3D spherically symmetric potential well

The Schrödinger equation describing the motion of a particle of mass m and energy E in a potential V which is a function of radius r can be solved exactly or approximately in terms of a spherically symmetric potential of various shapes. An example of one such potential is given in Fig. 1 with a finite depth $V(r)=-V_0$ for $r<a$, and $V(r)=0$ for $r\geq a$, where V_0 is positive, has been treated in many books [14–26]. A brief description of the analysis used in the present work is given in Appendix A. There, Eqs. (A.2) and (A.3) show that the calculations depend on m, the depth of the potential V_0 and $r=a$, which is taken as the thickness of the membrane, and the angular momentum quantum number ℓ. For the time being we will be interested in the case $\ell=0$ with the scattering center at the origin.

2.2. Bound states

Matching the two solutions (A.4) and (A.5) of the Schrödinger equation (cf. Appendix A) and their first derivatives at $r=a$, one gets

* Corresponding author. Tel./fax: +33 388 60 66 94.
E-mail address: sabry.elkomoss@laposte.net (S.G. Elkomoss).

1567-5394/$ – see front matter © 2008 Elsevier B.V. All rights reserved.
doi:10.1016/j.bioelechem.2008.03.002

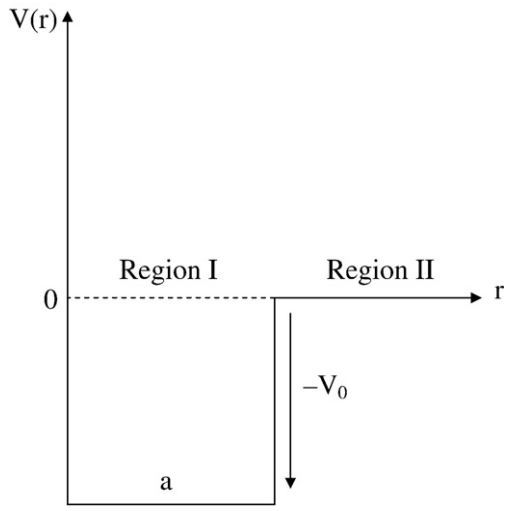

Fig. 1. Representation of the spherically symmetric square well potential of depth V_0 and radius a.

Eq. (1) that determines the eigenvalues $|E|$ of the bound states inside the well for $\ell=0$:

$$\cot\ \alpha a = -\beta/\alpha \tag{1}$$

where

$$\alpha^2 = 2m(V_0 - |E|)/\hbar^2 \text{ and } \beta^2 = 2m|E|/\hbar^2. \tag{2}$$

Eq. (1) is the same as that obtained for the odd parity of Eq. (8) for the 1D finite square potential well model of width $2a$ calculated in [1]. Eq. (1) (this work) as well as Eq. (8) in [1] have been solved graphically by different authors [20–22]. Instead of approximate graphical solutions, we have solved these equations numerically such that the difference between the left- and right-hand sides is less than 10^{-7}. As a matter of fact, for the case $\ell=0$, the 1D and 3D square potential wells are almost identical except that in the former the domain x is $-\infty$ to $+\infty$ in place of $0<r<+\infty$ and that the wave function R_0 is replaced by $\chi(r)=R_0(r)/r$. It is worth mentioning that in the 1D potential well one calculates the transmission coefficients T that vary between 0.0 and 1.0 [1], while the scattering cross sections are obtained with the 3D potential well used in this paper.

2.3. Phase shifts δ_0 and the elastic scattering cross section σ_0 for $\ell=0$

As in Section 2.2., taking $\ell=0$ with $E=-|E|$ and matching the two solutions of the Schrödinger equation and their first derivatives between the regions I and II of Fig. 1 at $r=a$, the phase shifts δ_0 are given by the expression:

$$\tan\ \delta_0 = [(k/\kappa)(\tan\ \kappa a) - (\tan\ ka)]/[1 + (k/\kappa)(\tan\ ka)(\tan\ \kappa a)] \tag{3}$$

where

$$\kappa^2 = 2m(V_0 + E)/\hbar^2 \text{ and } k^2 = 2mE/\hbar^2. \tag{4}$$

Eq. (3) is a multivalued function for which we will consider only the case $\pi/2<\delta_0<\pi$, where there is at least one s ($\ell=0$) bound state [14,19,23].The partial scattering cross section for $\ell=0$ is given by:

$$\sigma_0 = 4\pi k^{-2}\ \sin^2\delta_0. \tag{5}$$

More generally, the cross section σ_ℓ is given by:

$$\sigma_\ell = 4\pi(2\ell+1)k_\ell^{-2}\ \sin^2\delta_\ell. \tag{6}$$

Then the total cross section can be written as:

$$\sigma_{\text{tot}} = 4\pi\sum_{\ell=0}(2\ell+1)k_\ell^{-2}\ \sin^2\delta_\ell. \tag{7}$$

Since 1947 much work has been done on the inverse problem of the determination of the scattering potential from reflection coefficients and from phase shifts δ for $\ell=0$ or other ℓ values [27–33]. However, there is a question of how much a small change in the scattering potential V_0 changes E and σ_0. An answer for the HRBC membrane is given in Table 2 of Section 3.1. showing that for K^+ an infinitesimal change of V_0 indeed produces a change in $|E|$ and δ_0, and consequently σ_0 changes.

2.4. Permeability coefficient P

In Eqs. (3) and (1) in [1], the T and $(1-T)$ coefficients are given by the transmission and reflection amplitudes $|A/D|^2$ and $|F/D|^2$. In the 3D case it has been shown that the differential elastic scattering cross section is related directly to the scattering amplitude [19], i.e. $(1-T)$ and to the phase shifts. This means that as σ_0 increases, $(1-T)$ also increases and therefore P decreases. We can then conclude that P is inversely proportional to σ_0. In other words, the product $P\sigma_0$=constant, which as we shall see, seems to be a plausible assumption. Thus having calculated σ_0 for different ions and knowing P for one specific ion from the literature, we can determine P for any other ion. In addition, one can expect from the calculations of P in the 3D case and T in the 1D case that the change of P for different ions in various membranes occurs in the same direction as that of T for the corresponding ions in the same membranes, which agrees with [34]. Some of these calculations will be given in Section 3.1. It has to be mentioned that throughout this paper we have used the notation σ to represent the scattering cross section and not the reflection coefficient as is usually the case in the literature.

3. Results and discussion

3.1. Human red blood cell membrane

For this membrane the values of $V_0=-14.06$ mV and $a=5$ nm are the values that give the best agreement of σ_0 and P with the available experimental data. Taking the value of $P_{K+}=1.7\times10^{-12}$ m/s from [2] as reference and applying the simple relation as explained in Section 2.4., i.e.,

$$P_{X+}/P_{K+} = \sigma_{0K+}/\sigma_{0X+} \tag{8}$$

where P_{X+} is the permeability of the ion X^+ to be determined. In this way values of P for the different ions can be obtained. In Table 1 the

Table 1
Values of $|E|$, δ_0, σ_0, P_{calc} and P_{ref} for the ions HCO_3^-, Li^+, Cs^+, Cl^-, NH_4^+, K^+, Na^+ and Rb^+ with $V_0=-14.06$ mV and $a=5$ nm in the human red blood cell membrane

Ion	$\lvert E\rvert$(mV)	δ_0	σ_0 (m^2)	P_{calc} (m/s)	P_{ref} (m/s)
HCO_3^-	7.762	148.538	1.511×10^{-22}	1.630×10^{-11}	
Li^+	11.227	156.804	5.230×10^{-22}	4.710×10^{-12}	
Cs^+	2.197	124.381	6.126×10^{-22}	4.021×10^{-12}	
Cl^-	3.753	125.725	1.301×10^{-21}	1.893×10^{-12}	
NH_4^+	3.406	145.775	1.352×10^{-21}	1.822×10^{-12}	
K^+	4.607	94.592	1.449×10^{-21}	1.7×10^{-12}	1.7×10^{-12}[2]
Na^+	5.391	158.173	1.579×10^{-21}	1.560×10^{-12}	1.1×10^{-12}[3]
Rb^+	0.437	134.582	2.959×10^{-21}	0.832×10^{-12}	

calculated values of $|E|$, δ_0, σ_0, P_{calc} and P_{ref} are given in decreasing order of P for the permeant ions HCO_3^-, Li^+, Cs^+, Cl^-, NH_4^+, K^+, Na^+ and Rb^+. Table 1 shows that there is an excellent agreement between the calculated and experimentally obtained values of P. For instance, in [3] the P_{K+} is estimated to be of the order of 10^{-12} m/s and the maximum value of P_{Na+} is 1.1×10^{-12} m/s. One should notice that P_{HCO3-} is at least one order of magnitude greater than P_{K+} or P_{Na+}. Furthermore, P_{Na+} is smaller than P_{K+} or P_{Cl-}. More generally, the membrane selectivity for the ions considered here can be given as:

$$HCO_3^- > Li^+ > Cs^+ > Cl^- > NH_4^+ > K^+ > Na^+ > Rb^+. \quad (9)$$

Finally, the permeability obtained in the 3D model (Table 1) for HCO_3^-, K^+ and Na^+ decreases in order like T for the corresponding ions calculated in the 1D model of [1], which are 0.987, 0.498 and 0.413, respectively, with $V_0=-14$ mV, and $a=5$ nm. This confirms what was stated in Section 2.4. The values of Table 1 are self-consistent, that means, knowing the calculated values of σ_0 and taking the permeability of any ion among those in Table 1 as reference, one can get P for the other ions by using Eq. (8). Calculations are also carried out for $V_0=-10$, -14, -14.05 and -14.06 mV with $a=5$ nm. In Table 2 the values of V_0, $|E|$, δ_0 and σ_0 for these different values of V_0 are given for K^+. This table shows that a small decrease in the absolute value of V_0 leads to a decrease in $|E|$, an increase in δ_0 and consequently a change in σ_0. The values for σ_0 in Table 2, which differ from $\sigma_0=1.449\times10^{-21}$ m^2 obtained for K^+ with $V_0=-14.06$ mV and $a=5$ nm, fit less well with the values given in the literature as has been mentioned in Section 3.1.

It should be mentioned again that the calculated HRBC membrane permeability for different ions (Table 1) is based on the experimentally obtained permeability for K^+ under conditions where nearly all known specific ion transport pathways involving K^+ are inhibited or silent. The only still active specific ion transport pathway for K^+ is the $K^+(Na^+)/H^+$ exchanger [2]. Therefore, the calculated permeability coefficients reflect values closely related to the ground state HRBC membrane permeability for these ions. The experimentally estimated HRBC membrane permeability for Cl^- and other monovalent anions is several orders of magnitude higher because of the fast permeability of these ions via the anion exchanger (band 3 protein). The anion exchange and net permeability of the HRBC membrane is of the order of 10^{-5} m/s and 10^{-9} m/s, respectively. Therefore the values of the calculated anion permeabilities (this paper) cannot be compared with these high permeability coefficients.

3.2. Resting axolemma squid axon membrane

The experiments of Steinbach [7] and Steinbach and Spiegelman [8] suggested that the squid axon is permeable to Cl^-, Na^+ and K^+. In [9,10] the non-excised resting membrane is assumed to be permeable to K^+ and possibly Cl^- ions, but is only poorly permeable to Na^+. Data obtained indicate that P_{Cl-} is larger than P_{Na+} [9–12]. However, while the permeability of Na^+ is smaller than that of K^+, it is not negligible [10]. The ratio P_{Na+}/P_{K+}, as determined by different investigators, ranges between 0.04 and 0.10 [10–13] and the ratios $K^+/Na^+/Cl^-$ given by others are 1/0.04/0.45 [9]. In this case, taking the only available value $P_{K+}=1.8\times10^{-8}$ m/s [9], P_{Na+} would be in the range of 0.72×10^{-9} to 1.8×10^{-9} m/s and for the same permeability ratios 1/0.04/0.45, the $P_{Cl-}=8.1\times10^{-9}$ m/s. In the present paper, values of $V_0=-60$ mV and $a=8$ nm are used for the calculations of σ_0 and P. Taking as reference $P_{K+}=1.8\times10^{-8}$ m/s [9] and following the same procedure as in Section 3.1., one gets the calculated values of σ_0 and P for the ions K^+, Rb^+, Cl^-, Na^+ and NH_4^+ presented in Table 3, in decreasing order of P. This table indicates that the membrane selectivity for the ions considered can be given as:

$$K^+ > Rb^+ > Cl^- > Na^+ > NH_4^+ \quad (10)$$

which agrees with most of the references given above for this membrane. The calculated permeabilities also agree with literature data, although a better agreement could be obtained by varying V_0 and a as mentioned in Section 3.1.

Table 2
Variation of $|E|$, δ_0 and σ_0 for an infinitesimal change in V_0 with a=5 nm for K^+ crossing the human red blood cell membrane

$-V_0$ (mV)	$\lvert E\rvert$(mV)	δ_0	σ_0 (m^2)
10	1.007	142.174	2.508×10^{-21}
14	4.551	95.502	1.315×10^{-21}
14.05	4.597	94.737	1.479×10^{-21}
14.06	4.607	94.592	1.449×10^{-21}

Table 3
Calculated $|E|$, δ_0, σ_0, P_{calc}, P_{ref} and P_{calc}/P_{ref} for some permeant ions crossing the axolemma squid axon membrane with $V_0=-60$ mV and $a=8$ nm

Ion	$\lvert E\rvert$(mV)	δ_0	σ_0 (m^2)	P_{calc} (m/s)	P_{ref} (m/s)	P_{calc}/P_{ref}
K^+	2.580	173.038	0.383×10^{-22}	1.8×10^{-8}	1.8×10^{-8} [9]	1
Rb^+	2.430	157.517	1.849×10^{-22}	3.724×10^{-9}		0.207
Cl^-	4.860	157.509	2.231×10^{-22}	3.088×10^{-9}		0.172
Na^+	8.093	156.192	2.300×10^{-22}	2.994×10^{-9}		0.166
NH_4^+	5.929	105.735	2.275×10^{-21}	3.028×10^{-10}		0.017

4. Conclusion

The inequalities (9) and (10) show that the membrane selectivity for the same ions differs from one membrane to another. For example, the selectivity for K^+ is greater than for Cl^- in the resting axolemma squid membrane, whereas it is the inverse in the HRBC membrane. Eq. (8) shows that the relative permeability is equivalent to the inverse of the relative elastic scattering cross sections. In this case, the inequalities (9) and (10) can also be obtained from calculated values of σ_0. The good agreement between our calculated results and the data available in the literature is in favor of the plausible assumption of Eq. (8). Finally, carrying out measurements of the cross sections, applying the simple treatment developed in this paper and taking into account the phase shifts that correspond to $\ell=1$ and 2, more valuable information for ions in various membranes could be obtained.

Acknowledgement

One of the authors (S.G.E.) is deeply grateful to Anita Elkomoss for her continual support and encouragement since this work started.

Appendix A

It is impossible to obtain 3D analytical solutions of the Schrödinger equation for a spherically symmetric potential unless it can be separated into total differential equations in each of the three space coordinates (r, Θ, Φ). When separable, the wave function $\Psi(r,\Theta,\Phi)$ can be written:

$$\psi(r,\Theta,\Phi) = R_0(r)Y(\Theta,\Phi)/r \quad (A.1)$$

where $\chi=R_0(r)/r$ is the radial wave function solution for the particle moving in the attractive scattering potential $V(r)$, which falls off more rapidly than r^{-2} for large r. This restriction rules out scattering by the

Coulomb potential [23]. The radial Schrödinger equation for the two regions I and II of Fig. 1 can be written in the following forms:

$$\left(d^2\chi/dr^2\right) + \left[\alpha^2 - \ell(\ell+1)/r^2\right]\chi(r) = 0 \quad \text{for } r<a \tag{A.2}$$

$$\left(d^2\chi/dr^2\right) - \left[\beta^2 + \ell(\ell+1)/r^2\right]\chi(r) = 0 \quad \text{for } r\geq a \tag{A.3}$$

where α^2 and β^2 are given in Eq. (2) of the text. The solutions of Eqs. (A.2) and (A.3) for $\ell=0$ are:

$$\chi(r) = A\ \sin\ \alpha r \qquad \text{for } r<a \tag{A.4}$$

$$\chi(r) = \mathrm{Be}^{-\beta r} \qquad \text{for } r\geq a. \tag{A.5}$$

The boundary conditions at $r=a$, where Eqs. (A.4) and (A.5) and their first derivatives have to match, give Eq. (1) of the text that determines the eigenvalues $|E|$ of the bound states inside of the potential well for $\ell=0$.

Appendix B

With $E=-|E|$ and $\ell=0$, the solutions of Eqs. (A.2) and (A.3) are given by:

$$\chi(r) = C\ \sin\ (\kappa r) \qquad \text{for } r<a \tag{B.1}$$

$$\chi(r) = D\ \sin\ (kr+\delta_0) \qquad \text{for } r\geq a \tag{B.2}$$

where κ^2 and k^2 are given by Eq. (4) of Section 2.3 of the text and δ_0 is the phase shift for $\ell=0$. The boundary conditions of Eqs. (B.1) and (B.2) at $r=a$ determine δ_0, reported by different authors [14, 22], by the expression:

$$\delta_0 = \tan^{-1}((k/\kappa)\ \tan\ \kappa a) - ka. \tag{B.3}$$

Eq. (B.3) can also be written in the form of Eq. (3) of Section 2.3. of the text. Both Eqs. (B.3) and (3) are multivalued functions.

References

[1] S.G. Elkomoss, A. Pape, Calculation of transmission coefficients for some permeant molecules in human red cell and resting axolemma squid axon membranes, J. Biochem. Biophys. Methods 70 (2007) 525–530.
[2] R. Richter, J. Hamann, D. Kummarow, I. Bernhardt, The monovalent cation "leak" transport in human erythrocytes: an electroneutral exchange process, Biophys. J. 73 (1997) 733–745.
[3] L. Beaugé, V.L. Lew, Passive fluxes of sodium and potassium across red cell, in: J.C. Ellory, V.L. Lew (Eds.), Membrane Transport in Red Cells, Academic Press, New York, 1977, pp. 39–51.
[4] R. Motias, Organic anion transport in red blood cell, in: J.C. Ellory, V.L. Lew (Eds.), Membrane Transport in Red Cells, Academic Press, New York, 1977, pp. 197–220.
[5] I. Bernhardt, E. Weiss, Passive membrane permeability for ions and the membrane potential, in: I. Bernhardt, J.C. Ellory (Eds.), Red Cell Membrane Transport in Health and Disease, Springer-Verlag, Berlin, 2003, pp. 83–109.
[6] V.L. Lew, H.G. Ferreira, The effect of Ca on the K permeability of red cells, in: J.C. Ellory, V.L. Lew (Eds.), Membrane Transport in Red Cells, Academic press, New York, 1977, pp. 93–100.
[7] H.B. Steinbach, Chloride in the giant axon of the squid, J. Cell. Comp. Physiol. 17 (1941) 57–64.
[8] H.B. Steinbach, S. Spiegelman, The sodium and potassium balance in squid nerve axoplasm, J. Cell. Comp. Physiol. 22 (1943) 187–196.
[9] A.L. Hodgkin, B. Katz, The effect of sodium ions on the electrical activity of the giant axon of the squid, J. Physiol. 108 (1949) 37–77.
[10] S. Hagiwara, D.C. Eaton, A.E. Stuart, N.P. Rosental, Cation selectivity of the resting membrane of squid axon, J. Membr. Biol. 9 (1972) 373–384.
[11] P.F. Baker, A.L. Hodgkin, T.S. Shaw, The effects of changes in internal ionic concentrations on the electrical properties of perfused giant axons, J. Physiol. 164 (1962) 355–374.
[12] W.J. Adelman, Y.B. Fok, Internally perfused squid axon studied under voltage clamp conditions. II. Results. The effects of internal potassium and sodium on membrane electrical characteristics, J. Cell. Physiol. 64 (1964) 429–443.
[13] P.F. Baker, A.L. Hodgkins, H. Meves, The effect of diluting the internal solution on the electrical properties of a perfused giant axon, J. Physiol. 170 (1964) 541–560.
[14] R.G. Newton, Scattering Theory of Wave Particles, Dover Publications, New York, 2002. pp. 305-306.
[15] F. Calogero, Variable Phase Approach to Potential Scattering, Academic Press, New York, 1967.
[16] L.I. Schiff, Quantum Mechanics, McGraw-Hill, New York, 1955.
[17] D. Bohm, Quantum Theory, Prentice-Hall, Englewood Cliffs, NJ, 1951.
[18] D. Park, Introduction to the Quantum Mechanics, McGraw-Hill, New York, 1964.
[19] A.Z. Capri, Nonrelativistic Quantum Mechanics, 3rd ed.World Scientific, London, 2002.
[20] L.D. Landau, E.M. Lifshitz, Quantum Mechanics – Nonrelativistic Theory, Vol. 3, 3rd ed. Pergamon Press, New York, 1985.
[21] S. Gasiorowicz, Quantum Physics, 3rd ed.Wiley International Edition, 2003.
[22] N.F. Mott, S.W. Massey, The Theory of Atomic Collisions, 3rd ed.Clarendon Press, Oxford, 1965.
[23] B.H. Brandsen, Atomic Collision Theory, W. A. Benjamin, New York, 1970.
[24] R.A. Buckingham, The continuum, in: D.R. Bates (Ed.), Quantum Mechanics: I. Elements, Academic Press, New York, 1961, pp. 147–170.
[25] E.H.S. Burhop, Theory of collisions, in: D.R. Bates (Ed.), Quantum Mechanics: I. Elements, Academic Press, New York, 1961, pp. 299–436.
[26] P.M. Morse, H. Feshbach, Methods of Theoretical Physics, Vol. II, McGraw-Hill, New York, 1953.
[27] R. Jost, W. Kohn, Equivalent potentials, Phys. Rev. 88 (1952) 382–383.
[28] M.E. Moses, Calculations of the scattering potential from the reflection coefficients, Phys. Rev. 102 (1956) 559–567.
[29] V. Bargmann, Remarks on the determination of a central field of force from the elastic scattering phase shifts, Phys. Rev. 75 (1949) 301–303.
[30] V. Bargmann, On the connection between phase shifts and scattering potential, Rev. Mod. Phys. 21 (1949) 488–493.
[31] N. Levinson, Certain applied relationships between phase shifts and scattering potential, Phys. Rev. 89 (1953) 755–757.
[32] A. Martin, Analytic properties of $\ell \neq 0$ partial wave amplitudes for a given class of potentials, Nuovo Cim. 15 (1960) 99–109.
[33] A. Martin, On the analytic properties of partial wave scattering amplitudes obtained from Schrödinger equation, Nuovo Cim. 14 (1959) 403–425.
[34] G.B. Benedek, F.M.H. Villars, Physics with illustrative examples from medicine and biology, Statistical Physics2nd ed., Springer, New York, 2000 Chapter 2.